

# Ultrasensitive detection of dopamine using a polysilicon nanowire field-effect transistor†

Chih-Heng Lin,‡<sup>a</sup> Cheng-Yun Hsiao,‡<sup>a</sup> Cheng-Hsiung Hung,<sup>b</sup> Yen-Ren Lo,<sup>a</sup> Cheng-Che Lee,<sup>a</sup> Chun-Jung Su,<sup>b</sup> Horng-Chin Lin,<sup>b</sup> Fu-Hsiang Ko,<sup>c</sup> Tiao-Yuan Huang<sup>b</sup> and Yuh-Shyong Yang\*<sup>ad</sup>

Received (in Cambridge, UK) 28th July 2008, Accepted 9th September 2008

First published as an Advance Article on the web 1st October 2008

DOI: 10.1039/b812968a

**An unprecedented high sensitive sensing of neurotransmitter dopamine at fM level was demonstrated using a poly-crystalline silicon nanowire field-effect transistor (poly-SiNW FET) fabricated by employing a simple and low-cost poly-Si sidewall spacer technique, which was compatible with current commercial semiconductor processes for large-scale standard manufacture.**

Dopamine (DA) is an important neurotransmitter that modulates many aspects of brain circuitry,<sup>1</sup> influences a variety of motivated behaviors<sup>2</sup> and is involved in several neurological disorders,<sup>3–5</sup> including schizophrenia, Huntington's disease and Parkinson's disease (PD). As PD is characterized by a severe depletion of the *in vivo* DA pool, the ability to sensitively and selectively measure the concentration of the neurotransmitter DA could potentially be used for molecular diagnosis of PD. However, one of the primary problems is that the concentration of DA in the extracellular fluid of the caudate nucleus is extremely low for patients with PD.<sup>6,7</sup> The detection limit of the current techniques for DA is in the picomolar range.<sup>8–10</sup> A more sensitive approach is needed to detect DA directly and immediately, especially in neuronal communication research.

Semiconducting silicon nanowire field effect transistors (SiNW FETs) have been shown to function as a transducers for label-free, high-sensitivity and direct electrical detection of biomolecules.<sup>11–18</sup> The ultrahigh sensitive detection can be attributed to their small size and large surface-to-volume ratio, enabling local charge transfers to result in a current change due to a field effect, such as when the analytical molecules bind to specific recognition molecules at the surface of the nanowire. This effect is sufficiently strong that single charge at the surface of the nanowire can be sensed because the depletion or accumulation of charge carriers affects the entire cross-sectional conduction pathway of these nanostructures.<sup>19,20</sup>

Excellent electric properties of single-crystalline silicon nanowires (single-SiNWs) in a Bio FET transistor (single-SiNW FET as the transducer for biosensing) have been demonstrated.<sup>11–20</sup> However, single-SiNW FET for biological application has been seriously limited due to the difficulty in device manufacture process. Silicon nanowires (SiNWs) have been fabricated from various methods by either 'bottom up'<sup>11,21,22</sup> or 'top-down'<sup>12,23</sup> lithography approaches to form monocrystalline SiNWs channels of single-SiNW FET. The top-down approaches typically employ advanced optical or e-beam lithography tools to generate the NW patterns. Although compatible with mass-production, the use of advanced lithography tools with nanometer size resolution is costly. The bottom-up approaches usually employ metal-catalytic growth for preparation of NWs. The later approaches, however, suffer seriously from the difficulty in precisely positioning the device location. Metal contamination and control of structural parameters are additional issues that need to be addressed for practical manufacturing.

In addition to their proven performance in biosensing, how to mass produce NW FET devices, control their electronic properties and reduce the cost to a reasonable range will be the key aspects for their biomedical applications. For this reason, a simple and low-cost method to fabricate poly-crystalline silicon (poly-Si) NW FET for biosensing application has been demonstrated.<sup>24–28</sup> The poly-SiNW channel can be fabricated by employing the poly-Si sidewall spacer technique, in an approach which is compatible with current commercial semiconductor processes. Throughout the fabrication, no expensive lithography tools are needed for definition of the nano-scale patterns. The fabricated devices exhibited good performance and showed great potential to be developed to an ultrasensitive biosensor because of their excellent electrical characteristics in aqueous solution.<sup>29</sup> The purpose of this research is to further show that the poly-SiNW FET can function as a simple alternative to a transducer for ultra high sensitive biosensing of dopamine as shown in Scheme 1.

An n-type poly-SiNW FET device (Fig. 1A and B) with two poly-Si nano-channels, of 80 nm width and 2 μm length, fabricated based on our previously reported methods<sup>24–28</sup> was used as the transducer in this study and is described in Fig. S1 and S2 of ESI.† According to the fabrication process, each dummy-gate indirectly defined two NW channels that were connected to the source and drain pads (Fig. 1A). Also should be noted is the unique device structure, a significant portion of the poly-SiNW channel (a 80 nm width surface as

<sup>a</sup> Department of Biological Science and Technology, National Chiao Tung University, Hsinchu, 300, Taiwan.

E-mail: ysyang@faculty.nctu.edu.tw

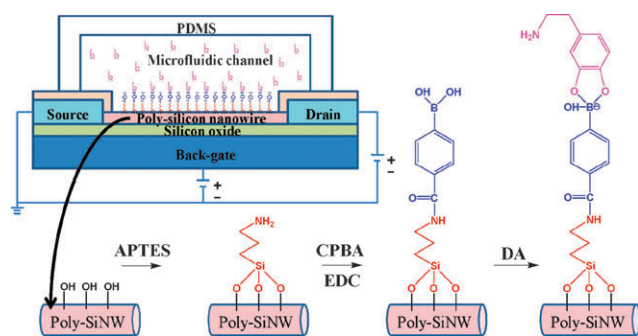
<sup>b</sup> Institute of Electronics, National Chiao Tung University, Hsinchu, 300, Taiwan

<sup>c</sup> Institute of Nanotechnology, National Chiao Tung University, Hsinchu, 300, Taiwan

<sup>d</sup> Instrument Technology Research Center and National Nano Device Laboratories, NARL, Hsinchu, 300, Taiwan

† Electronic supplementary information (ESI) available: Additional characterisation data. See DOI: 10.1039/b812968a

‡ C. H. L. and C. Y. H. contribute equally and are considered as joint first authors.



**Scheme 1** Functionalization of poly-SiNW for dopamine detection by poly-SiNW FET. Schematic illustration of poly-SiNW surface modification is shown. The poly-SiNW is housed in a PDMS microfluidic channel. Tungsten probe needles were connected to the source and drain pads and current changes were measured using three-probe contact geometries.

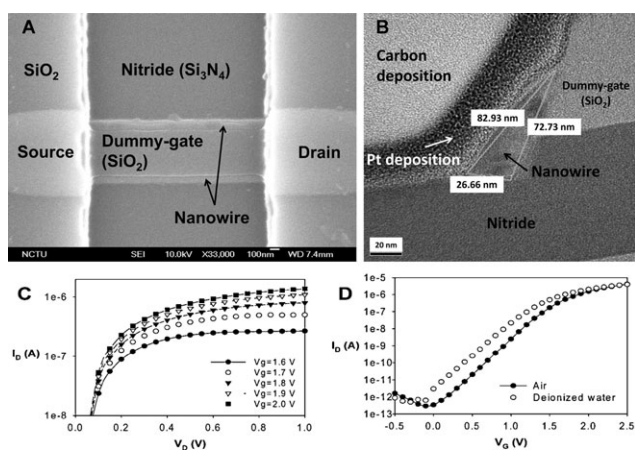


**Fig. 1** SEM image and electrical characterization of a poly-SiNW FET with two NW channels. (A) SEM image of the poly-crystalline SiNW FET. One dummy-gate was produced and indirectly defined two NW channels. The two NWs, 2  $\mu\text{m}$  in length, were connected to the source and drain pads. The SEM image is also illustrated in Fig. S2F of ESI.† (B) TEM cross-sectional view of the device. Pt and carbon deposition on the device were used to provide protection layers of the nanostructure under TEM sample preparation and for the purpose of enhancing the image contrast. The position of the TEM image is illustrated in Fig. S2E of ESI.† (C)  $I_D - V_G$  characteristics for  $V_G$  varied from 1.6 to 2.0 V with a step of 0.1 V. (D) Sub-threshold characteristics in air (●) and deionized water (○).

shown in Fig. 1B) was genuinely exposed to the environment. This lends itself nicely to chemical and biologic sensor applications, since the exposed channel region could serve as the sensing site.<sup>11,12</sup>

The high performance of the poly-SiNW FET device described above was verified by electrical characterization shown in Fig. 1C and D. All electrical measurements were taken with a Keithley picoammeter (4200A). The  $I_D - V_D$  characteristics were obtained by sweeping the source drain voltage while keeping the back gate voltage at a constant value. Output characteristics showed that the current of the device between the source and drain was controlled effectively by the gate electrodes as shown in Fig. 1C. Typical characteristics of the poly-SiNW FET at room temperature are shown in Fig. 1D. The  $I_D$  vs.  $V_G$  (from  $-0.5$  to  $2.5$  V) output characteristics with

constant  $V_D$  (0.5 V) exhibited excellent semiconductor FET characteristics, illustrating n-type behavior. Good device performance with high on/off current ratio (around 6 orders) turned on at low  $V_G$  (Fig. 1D) and reasonable sub-threshold swing ( $240$  mV decade<sup>-1</sup>) was achieved. It is of note that Si substrate capped with the 100 nm wet-oxide and 50 nm nitride layer was important to prevent the device from liquid invasion and retain its excellent electrical characteristics in aqueous solution<sup>28</sup> as shown in Fig. 1D (open circle).

In this study, we detect DA on the preferential binding of phenylboronic acid to DA.<sup>8,30</sup> As shown in Scheme 1, the resulting DA–boronate ester complex produces a negative charge that can greatly affect the surface conductivity of SiNW FET, which was used to transduce the binding events in this study. The boronic acid functionalized poly-SiNW was synthesized *via* a two-step reaction of surface modification: the amino group introduced by 3-aminopropyltriethoxysilane (APTES) was coupled to 4-carboxyphenylboronic acid (CPBA) under the activation of *N*-ethyl-*N'*-(3-dimethylamino-propyl)carbodiimide (EDC) as shown in Scheme 1. The PDMS micro-fluidic channel, which was made with acrylic, PDMS and metal holder, was placed on top of the device to hold the aqueous solution surrounded poly-SiNW (top Scheme 1). Fluorescent dye alizarin red S (ARS), which contains a diol group and is able to form a boronate ester with CPBA to emit fluorescent light, was used to confirm the results of functionalization on the surface of poly-SiNW (Fig. 2). Fluorescence cannot be observed without the modification described above on poly-Si surface (more detailed experimental procedures and controlled experiments given in Fig. S3 of ESI†).

Specific reaction between DA and CPBA immobilized on the poly-SiNW FET surface produces a negative charge (Scheme 1). For an n-type NW FET, a decrease of the current will be expected when negative charges were introduced on its sensing surface. Thus, the change of electrical signal of the FET device may reflect the amount of DA applied in the microfluidic channel. The DA sensing event was demonstrated and shown in Fig. 3. In these experiments, reagents in aqueous solution were loaded by syringe pump to the PDMS microfluidic channel that covers the SiNW surface. As shown in

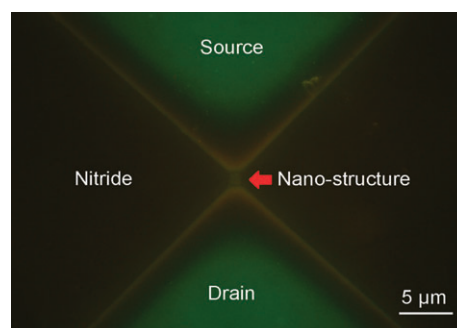


**Fig. 2** Fluorescent microscopic image of the functionalized poly-SiNW FET device following reaction with ARS dye. Detailed layout of the structure can be found in Fig. S1 of ESI.† The red arrow indicates the functionalized nano-structure which specifically captured ARS and emitted the fluorescent light under blue light excitation. The fluorescent intensity and colour were dependent on silicon thickness.

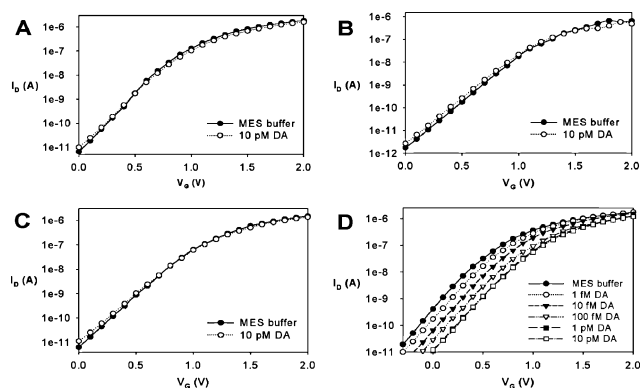


**Fig. 3** Responses of poly-SiNW FET to DA in aqueous solution. The solution contained 10 mM MES buffer at pH = 6.0. A constant  $V_D$  was set at 0.5 V. The electric responses were obtained in MES buffer (●) and in the presence of 10 pM DA (○). (A)  $I_D$ - $V_G$  curves obtained from unmodified poly-SiNW FET. (B)  $I_D$ - $V_G$  curves obtained from APTES modified poly-SiNW FET. (C)  $I_D$ - $V_G$  curves obtained from EDC and CPBA treated poly-SiNW FET. Only the completely functionalized (treated with APTES, EDC and CPBA) device (D) gave the expected binding responses upon titration of DA from 1 fM to 10 pM. The disparities in  $I$ - $V$  characteristics measured in MES buffer among the devices were attributed to the performance fluctuation, mainly due to the use of thick gate dielectric and the non-regular cross-sectional shape of the nanowires.<sup>32</sup>

Fig. 3A–C, without the complete functionalization on the SiNW surface with APTES, EDC and CPBA, the presence of DA gave similar  $I_D$ - $V_G$  curves to that obtained in MES buffer. These results indicate that non-specific binding of DA to SiNW did not occur. Fig. 3D shows the binding response of the completely functionalized poly-SiNW FET following titration with DA from 1 fM to 10 pM. The  $I_D$ - $V_G$  curves shown in Fig. 3D revealed that the electric response correlated with the DA concentration and saturated at 1 pM. This observation indicates that the change of current in the  $I_D$ - $V_G$  curve was specifically affected by the interaction between DA and boronate. A recently published method using an ion-sensitive FET (ISFET) as transducer gives the detection limit for DA at  $7 \times 10^{-5}$  M.<sup>30</sup> Using a similar scheme, the lowest detectable concentration (1 fM or  $10^{-15}$  M) obtained with poly-SiNW FET represented a powerful improvement for ultrasensitive detection with a nanoscale sensor. In the future, a CMOS detection circuit<sup>31</sup> can be integrated with poly-SiNW FET for ultrasensitive dopamine sensing.

In summary, we demonstrate for the first time, that semi-conducting poly-SiNW FET with thickness at nanometer scale and length at 2  $\mu$ m, could be developed to a highly specific sensor for neurotransmitter DA with sensitivity in the fM concentration regime. The ease of the device fabrication offers the advantages including (i) high uniformity and reproducibility, (ii) high yield, and (iii) excellent scalability and manufacturability. As DA sensors, the advantages of the poly-SiNW FET sensing device are (i) ultrasensitive and label-free, (ii) cost-effective, (iii) rapid, direct, turbid and light absorbing tolerant, and (iv) potential for developing a portable, robust, low-cost, and easy-to-handle electrical component suitable for field test and homecare use. In addition, fabricating the poly-SiNW FET

by the proposed top-down approach makes it possible to produce SiNW FET of both low- and high-multiplexing capabilities and permits direct integration with electrical readout circuits. This would be of great scientific and commercial values and may open the door to direct gene profiling and molecular diagnostics.

This research is supported by National Science Council, Taiwan (97-2321-B-009-001 and 96-2120-M-009-001).

## Notes and references

- 1 S. Ikemoto, *Brain Res. Rev.*, 2007, **56**, 27.
- 2 J. R. Wickens, J. C. Horvitz, R. M. Costa and S. J. Killcross, *Neuroscience*, 2007, **27**, 8181.
- 3 S. R. Laviolette, *Schizophr. Bull.*, 2007, **33**, 971.
- 4 T. S. Tang, X. Chen, J. Liu and I. J. Bezprozvanny, *Neuroscience*, 2007, **27**, 7899.
- 5 J. E. Ahlskog, *Neurology*, 2007, **69**, 1701.
- 6 J. B. Justice, *J. Neurosci. Methods*, 1993, **48**, 263.
- 7 R. D. O'Neill, *Analyst*, 1994, **119**, 767.
- 8 S. R. Ali, Y. Ma, R. R. Parajuli, Y. Balogun, W. Y. Lai and H. He, *Anal. Chem.*, 2007, **79**, 2583.
- 9 T. Yoshitake, J. Kehr, S. Yoshitake, K. Fujino, H. Nohta and M. Yamaguchi, *J. Chromatogr. B: Anal. Technol. Biomed. Life Sci.*, 2004, **807**, 177.
- 10 M. Du, V. Flanigan and Y. Ma, *Electrophoresis*, 2004, **10**, 1496.
- 11 Y. Cui, Q. Wei, H. Park and C. M. Lieber, *Science*, 2001, **293**, 1289.
- 12 Z. Li, Y. Chen, X. Li, T. I. Kamins, K. Nauka and R. S. Williams, *Nano Lett.*, 2004, **4**, 245.
- 13 Z. Fan and J. G. Lu, *Appl. Phys. Lett.*, 2005, **86**, 123510.
- 14 R. J. Chen, H. C. Choi, S. Bangsaruntip, E. Yenilmez, T. Xiaowu, Q. Wang, Y. L. Chang and H. J. Dai, *J. Am. Chem. Soc.*, 2004, **126**, 1563.
- 15 T. I. Kamins, S. Sharma, A. A. Yasseri, Z. Li and J. Straznicki, *Nanotechnology*, 2006, **17**, S291.
- 16 M. W. Shao, Y. Y. Shan, N. B. Wong and S. T. Lee, *Adv. Funct. Mater.*, 2005, **15**, 1478.
- 17 E. Stern, J. F. Klemic, D. A. Routenberg, P. N. Wyrembak, D. B. Turner-Evans, A. D. Hamilton, D. A. LaVan, T. M. Fahmy and M. A. Reed, *Nature*, 2007, **445**, 519.
- 18 N. Elfström, R. Juhasz, I. Sychugov, T. Engfeldt, A. Eriksson Karlström and J. Linnros, *Nano Lett.*, 2007, **7**, 2608.
- 19 F. Patolsky, G. Zheng, O. Hayden, M. Lakadamyali, X. Zhuang and C. M. Lieber, *Proc. Natl. Acad. Sci. USA*, 2004, **101**, 14017.
- 20 F. Patolsky, G. Zheng and C. M. Lieber, *Nanomedicine*, 2006, **1**, 51.
- 21 X. Duan, Y. Huang and C. M. Lieber, *Nano Lett.*, 2002, **2**, 487.
- 22 M. C. McAlpine, R. S. Friedman, S. Jin, K. H. Lin, W. U. Wang and C. M. Lieber, *Nano Lett.*, 2003, **3**, 1531.
- 23 K. N. Lee, S. W. Jung, W. H. Kim, M. H. Lee, K. S. Shin and W. K. Seong, *Nanotechnology*, 2007, **18**, 445302.
- 24 H. C. Lin, M. H. Lee, C. J. Su, T. Y. Huang, C. C. Lee and Y. S. Yang, *IEEE Electron Device Lett.*, 2005, **26**, 643.
- 25 C. J. Su, H. C. Lin and T. Y. Huang, *IEEE Electron Device Lett.*, 2006, **27**, 582.
- 26 C. J. Su and H. C. Lin, *IEEE Trans. Nanotechnol.*, 2007, **6**, 206.
- 27 C. J. Su, H. C. Lin, H. H. Tsai, T. M. Wang, T. Y. Huang and W. X. Ni, *Nanotechnology*, 2007, **18**, 215205.
- 28 C. Y. Hsiao, C. H. Lin, C. H. Hung, C. J. Su, Y. R. Lo, C. C. Lee, H. C. Lin, F. H. Ko, T. Y. Huang and Y. S. Yang, *Biosens. Bioelectron.*, 2008, DOI: 10.1016/j.bios.2008.07.032.
- 29 H. C. Lin, C. J. Su, C. Y. Hsiao, Y. S. Yang and T. Y. Huang, *Appl. Phys. Lett.*, 2007, **91**, 202113.
- 30 R. Freeman, J. Elbaz, R. Gill, M. Zayats and I. Willner, *Chem.–Eur. J.*, 2007, **13**, 7288.
- 31 F. L. Chan, W. Y. Chang, L. M. Kuo, C. H. Lin, S. W. Wang, Y. S. Yang and M. S-C Lu, *J. Micromech. Microeng.*, 2008, **18**, DOI: 10.1088/0960-1317/18/7/075028.
- 32 Y. Cui, Z. Zhong, D. Wang, W. U. Wang and C. M. Lieber, *Nano Lett.*, 2003, **3**, 149.